Predicting natural attenuation of xylene in groundwater using a numerical model

---

Description of the simulations provided with the TBC demo input file

Abstract

The aquifer beneath an abandoned refinery in the Lower Rhine area, Germany, was contaminated with a number of different mineral oil products. Groundwater sampling in the area around the former xylene plant revealed that a xylene plume had developed in the underlying groundwater, and moreover, that there is strong evidence for in situ microbial xylene degradation with oxyegn, nitrate, sulfate and ferric iron as electron acceptors. In order to prevent further xylene spreading three pumping wells extracting contaminated water were installed downgradient of the spill zone. The numerical reactive transport code TBC was applied to this situation to quantify the relation of microbial degradation to xylene removal by the pumping wells. It could be shown that the unamended in situ degradation was an appreciable xylene removal process that contributed to about one third to the total xylene removal (degradation plus extraction). A further objective of the model application was to predict xylene spreading under regional flow conditions, i.e. without operation of the three pumping wells, to consider the possible effects of natural xylene attenuation. To accomplish this the model calibrated for the situation with operating wells was transferred to the hydraulic situation of regional flow while retaining the parameters of the biochemical model. It turned out that the xylene plume that is expected to develop downgradient of the source area will be limited to an extension of not more than one thousand meters. An interesting feature of the simulations results was that xylene degradation under iron reducing conditions, which was of minor importance for the situation with operating pumping wells, becomes the dominant degradation mechanism under regional flow conditions. Moreover, iron reduction

will be the key process in controlling plume evolution. The model application illustrates that multi-species reactive transport models are needed to adequately transfer reactive processes from one hydraulic situation to another, while single species models are not suited for this predictive task.

1. Introduction

Aquifer contamination with mineral oil products is a widespread environmental problem. In Germany the maximum allowable concentrations for the sum of dissolved hydrocarbons in drinking water is 0.01 mg/l. On the other hand there is clear evidence that many mineral oil products like benzene, toluene and the xylene isomeres (BTX) are often subject to microbially mediated degradation in soils and aquifers. Aerobic BTX degradation in the field has been observed, for example, by Borden et al. (1995), MacIntyre et al. (1993), and Vroblesky and Chapelle (1994). Degradation of BTX-compounds in anaerobic aquifers with nitrate, iron(III), or sulfate as terminal electron acceptors (oxidants) is described by Barbaro et al. (1992), Cozzarelli et al. (1995), Thierrin et al. (1995), and Hunkeler et al. (1999). Evidence of BTX degradation could even be observed under fermentative and methanogenic conditions (Acton and Barker, 1992, Hunkeler et al., 1999).

An interesting empirical study on subsurface contamination was published by Hadley and Armstrong (1991). They examined nearly 3000 public water supply wells in California and found that benzene was detected in only 9 of these wells (0.3 %) although there is an estimated number of several thousands of leaking storage tanks in California which represent potential benzene contamination sources. Furthermore the generally less degradable tetrachloroethene was found in 200 wells (7 %), even though there are fewer potential sources for this compound.

The numerous field studies on the fate of BTX compounds in aquifers and the aforementioned data compilation suggest that a rather efficient degradation of those mineral oil products in aquifers (also called intrinsic bioremediation or natural attenuation) can be expected. Consequently the degradation potential of aquifers should be considered in risk analysis and contaminant transport predictions. Otherwise the hazardous potential of these compounds might be overestimated.

The present paper deals with xylene degradation in a sandy aquifer underlying an abandoned refinery in Germany. Its objective is to demonstrate the application of the numerical reactive transport model TBC (**T**ransport **B**iochemisty **C**hemistry, (Schäfer et al., 1998)) as a key tool in predicting future contaminant spreading for a real field situation. After a brief site description and case history the calibration of the model for a pump-and-treat remediation period is presented. Then the model is used to transfer the calibrated parameters to the actual aquifer situation with natural flow conditions which developed after the shut-down of the remediation wells. Finally the effect of xylene degradation on possible plume evolution is illustrated by means of two transport scenarios.

The first simulations for the field case under consideration were presented by Schäfer and Therrien (1995). However, the modelling at that time was restricted to the processes of aerobic and denitrifying xylene degradation and the evaluation of the pump-and-treat remediation period. The present simulations are based on the previous results and are extended in terms of additional important redox processes. Moreover the emphasis was completely changed between the two model approaches. While the main objective of the previous modelling was to quantify the contribution of microbial degradation to total xylene removal under pump-and-treat conditions, the motivation for the present simulations was to predict long-term xylene migration under natural (post-remediation) flow conditions. The extension of the reaction model was a prerequisite to accomplish this goal.

2. Site description and case history

The subsurface of a former xylene plant which was part of an abandoned refinery in Western Germany was partly contaminated with different mineral oil products. The dissolved contaminants were composed of about 80 % m- and p-xylene, 5 % o-xylene, 10 % ethylbenzene and of 5 % toluene and further unidentified aromatic compounds. The following simulations will consider the xylene isomers and ethylbenzene only. For simplification, the term xylene is used to denote the sum of the four compounds, which all have the same molecular formula.

The contaminated aquifer consists of calcite-rich quaternary fluvial sands. The saturated thickness varies between 14 m and 16 m, the distance to water table between 6 m and 8 m.

The groundwater surface is unconfined. After detection of the underground contamination in the mid 1980s the soil above the groundwater table was excavated and treated off site. The area was refilled with uncontaminated sand. Unfortunately the groundwater table at that time was relatively high and an appreciable amount of contaminants still remained in the subsurface below the groundwater table. These contaminants produced a plume of dissolved aromatic hydrocarbons in groundwater.

In May 1988 three pumping wells (R41.2, R41.3, and R41.4) were installed downstream of the spill area to prevent further dissolved contaminant spreading. The wells were screened in the upper 5 meters of the saturated zone only as it was expected that the contamination arising from the lighter-than-water aromatic hydrocarbon phase will mainly affect the upper part of the aquifer. This assumption was confirmed by two soil cores which were drilled in the vicinity of the spill area (HPC, pers. communications)

In 1990 the dissolved concentrations of selected hydrocarbons, oxygen, nitrate, sulfate, ferrous iron, calcium and the alkalinity were determined for 28 sampling points surrounding the spill area (HPC, 1991). Additionally, soil material in the source area close to the groundwater table was analyzed with respect to xylene content (HPC, 1992b). Fig. 1 shows the location of the abandoned refinery together with a detailed view of the former xylene plant, the approximate extension of the spill, and the positions of the sampling points.

In fig. 2 the results from 1990 groundwater and soil sampling are illustrated for the most important species. The measured xylene content of the soil material in the source region was rather high in the vicinity of the groundwater table. Maximum contents of about 70 g of xylene per kg dry soil (about 40 % equivalent saturation) imply that xylene is still present in the form of a presumably immobile light, non aqueous-phase liquid (LNAPL). Dissolved xylene concentrations are also enhanced in the spill area, and a xylene plume has evolved following the direction of groundwater flow. Dissolved oxygen and nitrate concentrations display an opposite behaviour. Their concentrations are relatively high outside the contaminated area, while they are significantly lower inside. Dissolved sulfate concentrations show a similar trend, however with a less pronounced concentration decrease. Dissolved iron concentrations are negligible outside the contaminated area, while they increase up to 25 mg/l inside. Not shown are calcium concentrations and the alkalinity, which are both higher within the contaminated area.

The pattern observed for the reactive species distribution together with knowledge on the general flow situation suggests the following hypothesis on reactive transport processes in the aquifer: The gradual dissolution of xylene present in the form of a residual LNAPL produces a xylene plume in groundwater. However, dissolved xylene does not only migrate with the groundwater, but it is also degraded in the aquifer. Dissolved oxygen, nitrate, sulfate and ferric iron associated with the aquifer material act as electron acceptors. The oxidation process is most likely mediated by heterotrophic microorganisms. The microbial production of inorganic carbon and subsequent calcite dissolution lead to an increase in calcite concentrations and in alkalinity. Meanwhile, enhanced microbial activity in the contaminated part of the aquifer sustained by different metabolic groups has been verified experimentally in the field by Zarda et al. (1998)

Following the hypothesis on reactive processes, xylene attenuation due to microbial degradation plays an important role for xylene fate in the aquifer. In particular, it can be expected that xylene propagation under natural flow conditions might be strongly affected by degradation processes. These considerations motivated the following model study, which emphasizes the quantification of the different degradation processes and the prediction of longer range reactive xylene transport under regional flow conditions based on the insights gained in the reactive processes under pump-and-treat conditions.

3. Model calibration for the remediation situation

Model calibration was performed for the same period as for the previous calibration (Schäfer and Therrien, 1995), i.e. the pump-and-treat remediation period which lasted from May 1988 (beginning of the pumping activities) through November 1992 (complete change in well configuration). The most important criterion to evaluate the quality of the calibration was the comparison between measured and simulated xylene concentrations at the three remediation wells. In addition, the simulated concentration distributions of the reactive species were compared to the results from the August 1990 sampling event (see fig. 2).

3.1 The TBC model

The partially screened wells installed for pump-and-treat remediation induce appreciable vertical flow in their vicinity. Moreover the non uniform vertical distribution of the LNAPL will result in preferential contamination of the upper part of the aquifer and, in consequence, in a non uniform vertical distribution of all reactive species. Therefore a realistic representation of groundwater flow and species distribution in the models cannot be achieved with a depth-averaged two dimensional model, but requires a fully three dimensional approach.

The multi-species reactive transport model TBC (**T**ransport, **B**iochemistry and **C**hemistry) was used to simulate xylene spreading in the aquifer. TBC allows for the numerical simulation of microbial growth according to Monod-type kinetics, subsequent microbial contaminant degradation with different electron acceptors and chemical reactions (kinetic and equilibrium reactions) coupled to three dimensional saturated groundwater flow and multi-species transport. Flow and transport equations are discretized with a finite element technique (Therrien and Sudicky, 1996), while the GEAR solver (Hindmarsh, 1974) is used to integrate the stiff set of ordinary differential equations describing the biochemical reactions. The equation system of the chemical reactions is solved with a Newton-Raphson method. Transport and reactions are sequentially coupled via an iterative multi-step method. Details on the TBC model and the coupling method can be found in (Schäfer et al., 1998).

The novel feature of TBC is that it is not limited to a given set of reactions. Instead the model provides reaction tools which comprise different reaction equations in a general form and which can be assembled by the user to a reaction model best fulfilling the requirements of a specific field or laboratory situation. TBC is therefore a very flexible model with a wide range of possible applications including in situ bioremediation, natural attenuation (intrinsic biodegradation), degradation studies in laboratory columns and early diagenetic processes in lake sediments. In addition to the biochemical and chemical reactions, TBC can also consider exchange processes between the different phases in an aquifer such as mobile pore water, immobile aquifer material, immobile biophase, and an immobile (residual) non aqueous phase liquid (NAPL).

3.2 Discretization and boundary conditions

Fig. 3 shows the model grid, the extension of the LNAPL, and the locations of the three remediation wells. The central part of the model domain is fine-spaced with a distance of 10 m between the nodes. This central area is surrounded by coarser cells in order to minimize boundary effects on simulation results in the area affected by the xylene spill. The largest spacing is 100 m. The model domain was resolved by six layers in the vertical direction. The thicknesses of the individual layers increase from 0.2 m for the top layer at the groundwater surface to 5 m for the lowest layer at the aquifer bottom. The horizontal discretization is the same for all six layers. The model grid is oriented such that two sides coincide with streamlines estimated from the observed head distribution, while the other two sides follow isolines of piezometric heads. The bottom face of the model is assumed to be impermeable, and the top face is formed by the water table. Groundwater recharge is applied to the top face.

The concentrations of the reactive species in the inflowing groundwater were provided from five sampling points located near the upstream model boundary (HPC, 1991). The reactive species concentrations in the recharging water were estimated to be 10 mg/l for dissolved oxygen, and 40 mg/l for sulfate, while it was assumed to be free of nitrate, dissolved iron and dissolved xylene. No mass exchange was simulated across the streamline boundaries of the flow model and across the bottom and top faces (except for species dissolved in groundwater recharge).

The only source for xylene in groundwater was dissolution from the immobile LNAPL. The horizontal extension of the area affected by LNAPL was given by observations, while the vertical extension in the saturated aquifer had to be determined during model calibration (see next chapter). The recent calibrations suggest that an initial mass of 65 t of xylene is in contact with the flowing groundwater. No observations on the iron content of the aquifer material were available. Therefore a typical value for quaternary sandy aquifers of 10 g/kg was assumed in the model (Scheffer/Schachtschabel, 1998).

3.3 Groundwater flow, solute transport and xylene dissolution

The hydraulic parameters for the flow model had been determined during independent measurements or were estimated from regional data. A uniform mean transmissivity was used for the whole model domain. It was derived from a number of pumping tests performed at the abandoned refinery (HPC, 1992a). A slight anisotropy of the aquifer was assumed with the vertical hydraulic conductivity being 2.5 times less than the horizontal conductivity. The mean annual recharge for the flat area with its sandy soils covered by grass lands was estimated to be 200 mm. This value corresponds to about 25 % of the mean annual precipitation in that region. Piezometric heads were periodically recorded since 1988, which allowed a reliable determination of the local flow system. An important feature was that the water table showed large temporal variations, while the mean flow direction was nearly time invariant. The water budget for the flow model revealed that 90% of the water entering the model domain is provided by boundary influx and only 10% is supplied by groundwater recharge in the model area.

No measurements were available for the effective porosity of the aquifer and the macro-dispersivities. The effective porosity could be estimated from the initial xylene concentrations at the different remediation wells and the knowledge on the approximate spill date. The dispersivities were adapted during model calibration. However, the model results were rather insensitive to changes in longitudinal and horizontal transverse dispersivity values as solute transport during the calibration period was characterized by near steady state conditions (see next chapter). The value for the longitudinal dispersivity was taken from the previous calibration, while transverse dispersivities were decreased in the recent calibration. This was done in order to prevent overestimation of xylene degradation due to transverse mixing for natural flow conditions (see chapter 5).

Furthermore the mean pumping rates had to be slightly modified as a more complete data base was available now. The flow and transport parameters used in the model are displayed in table 1.

The dissolution rate of LNAPL-xylene is a function of the contact area between the LNAPL body and the flowing groundwater. This contact area in turn depends on several factors including the elevation of the groundwater table. The groundwater table in the model area varied appreciably during the simulation period (Schäfer and Therrien, 1995).

8

Besides the macroscopic effect of groundwater table fluctuations, the phase exchange is also controlled by pore scale processes. Xylene is exchanged from the LNAPL into the groundwater by molecular diffusion. As this is a slow process, the maximum aqueous solubility of xylene will only be fully achieved for large surface areas of the xylene phase and for small groundwater flow velocities (e.g. Fried et al., 1979). However, in case of e.g. aggregated LNAPL-droplets and a generally patchy LNAPL distribution or for higher flow velocities, the mean xylene concentration in that part of the aquifer affected by the LNAPL might be appreciably lower than the maximum solubility (e.g. Powers et al., 1992). The spatial resolution of a field scale groundwater model does not allow one to resolve the small scale LNAPL distribution. Moreover this distribution will usually not be known in detail. Therefore a macroscopic kinetic approach has to be employed to account for the effect of limited phase exchange and the non-uniform LNAPL distribution. In TBC, a linear exchange kinetic model is used with the so-called exchange coefficient as an effective parameter.

While the time-dependent contact of the LNAPL with the flowing groundwater was taken from the previous calibration (Schäfer and Therrien, 1995), the value for the exchange parameter had to be slightly increased to compensate the effects from decreased transverse dispersivities used during the actual calibration. The exchange parameters are listed in table 1.

Sensitivity analysis showed that model results were very sensitive to changes in the value of the LNAPL exchange parameter. This value can usually not be determined independently. Therefore the model calibration for the smaller scale remediation situation was essential for a reliable prediction of xylene spreading under natural flow conditions.

3.4 Reactive processes

According to the afore mentioned hypotheses regarding the biochemical reactions affecting xylene transport, the following microbially mediated xylene degradation processes were considered in the model:
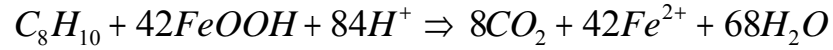
- Xylene degradation coupled to oxygen and nitrate reduction (Degradation reactions 1 and 2)

$$C_8H_{10} + 10.5O_2 \Rightarrow 8CO_2 + 5H_2O$$

$$C_8H_{10} + 8.4NO_3^- + 8.4H^+ \Rightarrow 8CO_2 + 4.2N_2 + 9.2H_2O$$
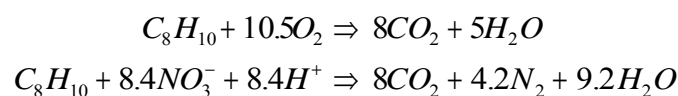
- Xylene degradation coupled to sulfate reduction (Degradation reaction 3)

$$C_8H_{10} + 5.25SO_4^{2-} + 5.25H^+ \Rightarrow 8CO_2 + 5.25HS^- + 5H_2O$$
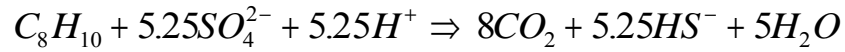
- Xylene degradation coupled to iron reduction (Degradation reaction 4):

$$C_8H_{10} + 42FeOOH + 84H^+ \Rightarrow 8CO_2 + 42Fe^{2+} + 68H_2O$$

It was assumed that reactions 1 and 2 were mediated by a single microbial group which is able to switch between aerobic and denitrifying metabolism. Reaction 3 is catalyzed by sulfate reducing bacteria and reaction 4 by iron reducing bacteria.

Additionally, it was considered in the model that the production of carbon dioxide and the consumption of protons in connection with the microbial activity will shift the calcite equilibrium of the groundwater:

$$CaCO_3 + CO_2 + H_2O \Leftrightarrow Ca^{2+} + 2HCO_3^-$$
$$HCO_3^- + H^+ \Leftrightarrow CO_3^{2-}$$
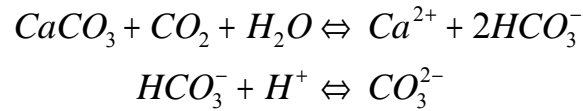
Finally the microbially produced sulfide and ferrous iron might form iron sulfide precipitates:

$$Fe^{2+} + S^{2-} \Leftrightarrow FeS\downarrow$$
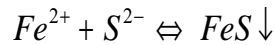
The observed enhanced ferrous iron concentrations together with the high alkalinity should promote the precipitation of iron carbonate (siderite). However, calculations with the equilibrium speciation model PHREEQE (Parkhurst et al., 1980) showed that the ambient groundwater was supersaturated with respect to siderite. Obviously siderite precipitation is proceeding very slowly. It was completely ignored in the model.

Xylene degradation was implemented in the TBC model in the form of microbially mediated kinetic reactions, while the dissociation and precipitation processes were treated as fast or equilibrium reactions.

During the four and a half year period used for model calibration, the total xylene content of the aquifer decreased only slightly. Additionally, the mean flow direction and pore water velocities remained nearly constant during this period. This implies that almost steady state conditions prevailed for xylene dissolution, transport, and degradation. Therefore model results have not been sensitive with regard to changes in the microbial growth and decay rates and yield coefficients. Standard rate values for groundwater environment have been adopted. The most sensitive parameters were the Monod-constants for xylene and for the dissolved oxidants and the microbial availability of the iron minerals. All biochemical parameters for

the microorganisms are displayed in Tables 2 and 3. The notation of the parameters are the same as those used in (Schäfer et al., 1998). Here one can also find more details on their role in the biochemical model.

The Monod-constants for oxygen and nitrate are low to allow for the nearly complete degradation observed for these two oxidants. In contrast, the observed sulfate reduction was less complete. This is reflected in increased Monod-constants for sulfate and xylene. The availability of the iron minerals was controlled by a limited exchange between the biophase which hosts the microorganisms and the mineral phase. This limited exchange was realized by adopting a low value for the exchange coefficient. Higher exchange coefficients would have rendered the solid iron better available for the iron reducers enabling them to consume all dissolved xylene, which is not in accordance with the observations. Moreover, an enhanced iron reducing activity would also have resulted in too high ferrous iron concentrations. The exchange processes between the biophase and the pore water have been considered to proceed instantaneously.

In addition to the afore mentioned degradation processes, a certain retardation should be expected for dissolved xylene. However, no independent observations on the retardation behaviour of xylene in that particular aquifer were available. Furthermore the quasi-steady state conditions did not allow the determination of a retardation factor during model calibration. A moderate retardation factor of 2.9 was assumed in the model. This value corresponds to an adsorption coefficient (k_d) of 0.3 l/kg. The adsorption coefficient was derived from a distribution coefficient for xylene between water and organic carbon (k_{OC}) of 300 (kg/kg) (Montgomery and Welkom, 1990) and an estimated fractional organic carbon content of the aquifer (f_{OC})of 0.001 by:

$$k_d = k_{OC} \, f_{OC}$$

3.5 Calibration results

Fig. 4 shows the measured and simulated xylene concentrations for the three remediation wells. The concentrations exhibit the typical trend for hydraulic remediation schemes. A pronounced decrease in concentrations can be observed during the first weeks of the well operations, especially for well R41.3 which is located closest to the contaminant source. In this initial phase the wells extract mainly pore water which has been in contact with the

11

LNAPL under regional flow conditions where lower pore water velocities prevailed. The velocities are then increased due to the well operations. While the exchange rate between LNAPL and pore water remains nearly constant, the dissolved xylene concentrations become lower because the mass of xylene dissolving in a given time increment is diluted into a larger groundwater volume. This effect is mainly responsible for the observed initial concentration decrease. After this initial phase a new equilibrium state is achieved at lower xylene concentrations. During this period xylene concentrations decrease only very gradually as the LNAPL forms a huge, long lasting reservoir. The observed concentration fluctuations are most probably caused by variable groundwater tables (see chapter 3.3) and variable pumping rates.

The simulated xylene concentrations are very similar to those from the previous calibration (Schäfer and Therrien, 1995). This is due to the fact that only minor changes were made for the hydraulic and hydrogeological model parameters and that total xylene degradation remained the same. The major difference between the two calibrations consists in the two additional degradation processes considered in the recent model, i.e. xylene degradation due to sulfate and iron reducing microbial activity.

Fig. 5 shows the simulated concentration distributions of sulfate and ferrous iron for the top layer of the model aquifer for August 1990. These distributions have to be compared to the interpolated observations for the same date displayed in fig. 2. However, only the trends in concentrations should be compared, as the partially screened sampling wells together with the expected steep vertical concentration gradients in the aquifer make it difficult to compare absolute values. The main obstacle to a direct comparison is that the volume averaging process in connection with water sampling cannot be reproduced exactly in the model. Furthermore, decreased sulfate and increased ferrous iron concentrations can be observed on the right hand sides of the plots in fig. 2. These effects are caused by a paraffin spill located about 300 m away from the xylene spill. The paraffin spill was not considered in the model and consequently its effects on reactive species distribution are not reproduced in the model.

The more detailed simulation of subsurface xylene degradation accomplished by the consideration of all known relevant degradation processes in this aquifer allows for a more reliable transformation of the degradation processes from the situation under pump-and-treat conditions to the regional flow system (see chapter 4)

12

The comparison between measured and simulated xylene concentrations in fig. 4 shows that the modelled concentrations for reactive transport match the observations in all three wells. By comparing the results to the non-reactive simulations it becomes obvious that the effect of the xylene degradation is more pronounced for the two marginal wells R41.2 and R41.4 than for the central well R41.3. This effect can be explained by the fact that oxidant-rich uncontaminated water mixes with the xylene-contaminated plume water at the edges of the plume. This mixing promotes high degradation activity in the regions where the wells R41.2 and R41.4 are located. Well R41.3 is located in the center of the plume where the water is already depleted in oxygen, nitrate, and sulfate. Here iron reducing bacteria maintain xylene degradation at low rates only, and consequently the differences between reactive and non reactive simulations are less pronounced.

A mass balance for the calibrated model showed that xylene is degraded at a mean rate of 0.9 kg xylene / d. This rate is in the same order of magnitude as the extraction rate for xylene at the three pumping wells, which amounts to about 1.5 kg xylene / d. This means that in situ microbial xylene degradation which accompanies the xylene extraction by the remediation wells unintentionally, contributes considerably to the total xylene removal of the aquifer. One third of the total degradation can be attributed to the aerobic and denitrifying pathway respectively, while degradation by sulfate reducing bacteria contributes about 20 % to total degradation. Less than 10% of the total xylene degradation can be attributed to iron reducing bacteria. Their activity is restricted by the low availability of the iron minerals, while the dissolved oxidants profit from the increased mixing between contaminated and pristine water induced by the operation of the pumping wells.

4. Prediction of xylene transport under natural flow conditions

The continuous delivery of xylene from the LNAPL into the flowing groundwater leads to almost stagnant xylene concentrations observed in the remediation wells. The mass balance analysis suggests that xylene removal by hydraulic remediation is not very efficient and it would take probably tens of years to remove the spilled xylene from the aquifer by this method. On the other hand the observations and simulations of the reactive species concentrations also suggest that xylene is efficiently degraded in the aquifer. Therefore an

13

alternative to the hydraulic remediation measure could be to turn off the wells and rely on the intrinsic degradation activity of the aquifer.

A key issue concerning the expected natural attenuation is its efficiency, i.e. what travel distance is required until the dissolved xylene concentrations reach acceptably low values. This question is the background for the second part of the simulations presented in the following sections. Its objectives are to transfer the model parameters determined during the calibration just described to a more regional model of xylene transport under natural flow conditions. This model will then be used in a kind of risk-assessment to predict the trends in future xylene spreading with the remediation wells turned off.

4.1 Set-up of the regional model

First, the existing model grid had to be adapted to the new problem. Regional groundwater discharges into the small river Lippe about 1.6 km downgradient from the xylene spill area (see fig. 1). The model grid therefore had to be extended along the flow direction in order to be able to simulate long-range transport. On the other hand, the grid size could be reduced in the transverse direction, as uniform flow is assumed in contrast to the situation with remediation wells, where an appreciable radial flow component was induced by the pumping activities. The modified grid consists of 24 nodes in the x-direction and 110 nodes in the y-direction (parallel to the flow direction). A spacing of 10 m was chosen for the discretization of the whole model domain leading to a grid extension of 1100 m along the flow direction and 230 m in the transverse direction. This is the same resolution that was used for the central part of the smaller scale model for the pump-and-treat period. The vertical discretization was completely adopted from the model for the remediation period (6 layers with a spacing between 0.2 m and 5 m).

The mean regional hydraulic gradient is 0.06 %. The values for hydraulic conductivities, the dispersivities, the retardation factor, and the phase exchange parameters were taken from the simulations under remediation conditions (cf. tab 1). The effective porosity was increased from 0.25 to 0.3 as it can be expected that a larger part of the pore water will be involved in solute transport for the decreased flow velocities of the regional simulations compared to the situation with the operating wells. Instead of a variable, water table-dependent contact zone

between the LNAPL body and groundwater, a constant mean vertical LNAPL extension into the groundwater of 0.65 m was assumed.

Simulations were performed for two scenarios. In scenario I, only advective and dispersive transport in addition to LNAPL dissolution was assumed, while the reactive processes identified during the calibration under remediation conditions were added in scenario II. The simulations extend over a period of 24 years. This time span is sufficient for the dissolved xylene to reach the outflow end of the model domain if it is not degraded.

4.2 Non-reactive transport

The only mechanisms considered during this scenario were retarded advective and dispersive xylene transport and dissolution of LNAPL-xylene into the groundwater. The initial concentrations for the LNAPL-xylene were taken from the 1992 measurements. In a first approximation, the maximum solubility of xylene was employed as initial dissolved xylene concentrations in that part of the model domain affected by the LNAPL while zero concentrations were employed elsewhere. The simulations revealed that the xylene concentrations did not reach maximum solubility even with the decreased regional flow velocities. The initial guess therefore overestimates dissolved xylene concentrations.

Fig. 6 shows the location of the LNAPL-xylene in the regional model and also the positions of six virtual observation points. These observation points allow one to track xylene spreading in the aquifer. They are assumed to be screened over the whole depth of the model aquifer, i.e. the simulated concentrations at this virtual sampling points are depth-averaged. The observation points are equidistantly placed along the plume axis with the first point (P1) located 100 m downstream the edge of the spill area, the second (P2) at 200 m distance and so on.

The concentration behaviour of xylene at the sampling points during the 24 years of simulation is illustrated in fig. 7a. Xylene concentrations first rise to a maximum and then decrease gradually. Concentration values are mainly controlled by the exchange coefficient which was identified during the calibration under remediation conditions. The concentrations are much lower than the maximum solubility as the concentrations at the depth-averaged virtual sampling points represent a mixture of xylene rich water from the top part of the aquifer and xylene-free bottom water.

15

The initial concentration decrease is partly due to the fact that the initial dissolved xylene distribution in the spill area was assumed to be at maximum solubility (see above) while xylene concentrations resulting from the rate limited dissolution of the LNAPL are somewhat lower actually. In general the slight temporal decrease in xylene concentrations is the consequence of a complete removal of parts of the LNAPL source at the edges of the spill area when it is flushed with groundwater from the uncontaminated upstream aquifer.

The xylene concentrations show a slight tendency to decrease along the flow path due to groundwater recharge and transverse dispersion. However, it becomes obvious that depth-averaged xylene concentrations at the discharge area located approximately 1000 m downstream of P6 will still be in the order of 10 mg/l.

4.3 Reactive transport

For this scenario, in addition to advective and dispersive transport, xylene degradation was considered according to the reaction model calibrated for the remediation period. The parameters of the reaction model remained essentially unchanged (cf. tabs 2 and 3). The initial dissolved and LNAPL-xylene distributions were the same as for the non-reactive case presented before. Initial concentrations for the dissolved oxidants were averaged from the observations in the uncontaminated part of the aquifer (5 mg/l for dissolved oxygen, 25 mg/l for nitrate and 40 mg/l for sulfate). The same values were used for concentrations in the water entering the model domain by groundwater recharge or at the upstream boundary.

The value for dissolved oxygen in the recharge water was decreased compared to the model calibration to account for possible oxygen consumption by natural organic carbon which might become relevant on the regional scale. Furthermore, the recharge water was considered to contain nitrate in the regional model, while it was nitrate-free in the smaller scale model used for calibration. The motivation to use different nitrate inputs is that the immediate vicinity of the former xylene plant is not used for agricultural purposes and therefore no nitrate bearing fertilizers will be applied there. However, the major part of the regional model domain is agricultural land, and it is reasonable to assume a certain nitrate leaching there.

The temporal course of the xylene concentrations in the six sampling points for reactive transport is displayed in fig. 7b. The maximum concentration at P1 is 10 mg/l compared to 16

mg/l in the non-reactive case. Moreover, the concentration decrease along the flow path is much more pronounced in the reactive case. Accordingly the concentration differences between the two scenarios are largest for the most downgradient observation point P6. The concentration behaviour for the reactive case suggests that xylene will be substantially decreased by degradation reactions and that dissolved xylene concentrations will reach values well below 1 mg/l in the discharge area of the aquifer.

Another interesting point is the relative contribution of the different oxidants to total xylene degradation. While more than 90% of the overall degradation activity could be attributed to bacteria using the dissolved oxidants (oxygen, nitrate, sulfate) in the remediation period, now most part of xylene degradation is performed by iron reducing bacteria. At the end of the simulation period (i.e. after 24 years of reactive transport under natural flow conditions), the degradation rate of the iron reducing bacteria amounts to 0.8 kg xylene / d while it is only 0.7 kg xylene / d for the other three bacteria groups together. The relative contributions of the different degradation pathways for the remediation and the natural flow period are illustrated in fig. 8

The shift in the relative importance of the four metabolic pathways is caused by the different hydraulic conditions. During the remediation period the flux of dissolved oxidants into the contaminated area was largely increased by the pumping wells while the activity of the iron reducing bacteria was limited by the low availability of the iron minerals and the relatively small extension of the plume. Now, for regional flow conditions, mixing between xylene and the dissolved oxidants is considerably reduced. Degradation activity is mainly located at the upstream boundary of the spill and the top surface of the plume, where oxygen, nitrate and sulfate enter the contaminated area by advective regional flow and groundwater recharge. To a much lesser degree, a certain activity of aerobic, denitrifying, and sulfate reducing bacteria can be found at the remaining surface of the plume, where xylene and dissolved oxidants are only poorly mixed by diffusion and transverse dispersion.

However, the contact between dissolved xylene and iron minerals increases as xylene spreads under regional flow conditions. This increasing contact in turn facilitates the overall degradation activity of the iron reducing bacteria. A steady state situation arises when the total xylene degradation rate equals the xylene dissolution rate from the LNAPL. The extension of the plume which develops until this steady state is achieved is a function of both the dissolution rate and the degradation activity. As the iron reducers are the most important

xylene degraders for regional flow conditions, the availability of iron minerals becomes a key parameter for the prediction of xylene spreading. Fig. 9 shows the simulated xylene distribution for a vertical slice along the flow axis for both scenarios. While xylene has already migrated across the boundary of the model domain for the non-reactive case, it is permanently contained in a quasi-steady state plume for the reactive case.

Fig. 10 shows the concentrations for selected reactive species of scenario II after 24 years of simulation for the same vertical slice as in fig. 9. At the top one can see the distribution of aerobic and denitrifying bacteria. They are   predominantly located at a narrow interface at the upgradient side of the spill, where advective fluxes of dissolved oxygen and nitrate into the area of enhanced xylene concentrations occur. A thin layer with microbial activity is also found at the top of the plume, where dissolved oxygen and nitrate fluxes are induced by groundwater recharge. Microbial activity at the bottom side of the plume is so low that it is not visible here. Inside the plume, aerobic and denitrifying microbial growth is not possible as dissolved oxygen and nitrate are depleted there, while xylene as carbon and energy source is missing outside the plume.

The concentration distribution for dissolved oxygen presented below illustrates the anaerobic zone that develops inside and downgradient of the spill area. Dissolved oxygen is only gradually recharged by the infiltrating water at the top of the plume. A similar behaviour can be observed for nitrate, sulfate reducers and sulfate (not shown).

A completely different behaviour is displayed by the iron reducers in the model. Their growth is primarily limited by the low availability of ferric iron from iron minerals. In consequence they are almost equally distributed over the plume area. Their growth stops when the xylene concentrations fall below a given threshold value specified by the Monod-constant for xylene. Finally the simulated concentration distribution of dissolved ferrous iron further illustrates the anaerobic iron rich plume that develops downgradient of the spill area and that largely exceeds the area of enhanced xylene concentrations (compare fig. 9). The calculated ferrous iron concentrations are unrealistically high. The reason for this is most likely that precipitation of ferrous iron minerals like siderite ($FeCO_3$) or re-oxidation of ferrous iron are not considered in the model.

5. Discussion of results

The main objective of the present modelling study was to predict natural attenuation of xylene in the contaminated aquifer. Of course the predictions are accompanied by a variety of uncertainties. One concerns the total amount of microbially available iron minerals in the aquifer. There is an ongoing discussion on the microbial availability of naturally occurring trivalent iron minerals (e.g. Heron and Christensen, 1995; Lovley et al., 1994; Phillips et al., 1993). If only part of the bulk iron can be accessed by microbes, then there is a risk that the aquifer might become exhausted earlier than expected in the model. In consequence the xylene plume might extend over a larger distance than predicted.

Furthermore the real aquifer is heterogeneous with an unknown hydraulic conductivity distribution while a homogeneous distribution is assumed in the model. Possible long-range structures can promote preferential flow and therefore the maximum extension of the xylene plume might be underestimated by the homogeneous model.

An intrinsic model problem arises from numerical transverse dispersion which cannot be completely excluded in the TBC model. As mixing of xylene and dissolved oxidants is artificially increased by this effect at the edges of the plume the model will overestimate xylene degradation performed by the aerobic, denitrifying and sulfate reducing bacteria (Cirpka et al., 1999).

Another type of uncertainty concerns the final xylene concentrations. The bacteria will not completely oxidize xylene, but their activity will cease at a certain concentration level. So there is a risk that maximum final xylene concentration might partly exceed drinking water limits. Undesired metabolic products could also accumulate. However, a number of laboratory studies and detailed field scale investigations give rise to the expectations that biodegradation is a very efficient removal process for xylene.

Regarding the uncertainties in connection with the microbial availability of iron and numerical transverse dispersivity, the model results are probably not conservative, i.e. xylene degradation might be overestimated by the simulations. However, the model assumes that the exchange coefficient between NAPL-xylene and dissolved xylene is constant in time while it will decrease in reality when the LNAPL is gradually dissolved. This is the consequence of the fact that better accessible parts of the LNAPL will dissolve first leaving a LNAPL body with a continuously decreasing accessibility to the flowing groundwater (e.g. Holman and

Javandel, 1996; Imhoff et al., 1993; Powers et al., 1994). This process will generally lead to a lower xylene concentrations in the plume than predicted with the constant exchange coefficient model.

6. Conclusions

Reactive xylene transport has been simulated for two different situations. First the reactive transport model was calibrated against concentration data recorded during a 4.5 years long period of pump-and-treat remediation accompanied by natural xylene degradation. Then the calibrated model was used to predict future xylene spreading under regional flow conditions.

The simulation of xylene spreading during the remediation period has revealed that natural in situ degradation contributes substantially to total xylene removal from the aquifer. Here the success of the reactive transport model TBC was its ability to quantify the effect of enhanced oxidant flux induced by the wells into the contaminated area.

Even more important, the model allowed the transfer of parameters from the reaction model identified for the remediation period to the regional flow system where different hydraulic conditions prevail. Here the model results suggest that xylene spreading will be limited by an efficient subsurface degradation.

The mass balances for the reactive species showed that the relative contributions of the individual oxidants to total xylene degradation is completely shifted when the flow field is changed. While the iron reducers were of minor importance under remediation conditions, they became the most important bacteria for the regional flow situation.

It should be noted here that the effects of changing hydraulic conditions on xylene degradation could not have been simulated adequately using a single-species degradation model. Only more complex multi-species reactive transport models like the one applied here provide the capability to consistently transfer reaction rates from one hydraulic situation to another, because the effective rates in such models develop according to the sometimes complex interactions between flow, solute transport, aquifer composition and biochemical parameters.

Although the pump-and-treat remediation was assisted by in situ xylene degradation, its efficiency concerning the aquifer clean-up was low. This is mainly due to the presence of LNAPL-xylene in the top region of the aquifer. The simulation results suggest, however, that the expected in situ degradation would be sufficient to limit the extent of the xylene plume to a distance of less then 1000 meters downstream of the spill area. Therefore relying on the intrinsic bioremediation is a real alternative to pump-and-treat remediation in this case. This is also reflected by the result that the simulated in situ xylene degradation rate under natural flow conditions (1.5 kg xylene / d) equals the xylene extraction rate achieved by the three remediation wells.

In the case presented here the authorities decided in 1996 to allow for a cessation of the remediation activities and to rely on the degradation potential of the aquifer. The xylene concentrations are continuously monitored, but, owing to the low groundwater flow velocities, it will still take a couple of years until the model predictions can be evaluated with the help of measured data. In any case one must be aware that groundwater quality will always be deteriorated by the xylene contamination, because even for very efficient xylene degradation e.g. the dissolved iron content of the groundwater will rise well beyond the threshold values for drinking water (0.2 mg/l total iron in Germany).

The decision of the authorities is corroborated by the findings of this study. The successful implementation of the model in this case points out that the assessment of natural attenuation is an important field of application for multi-species reactive transport models. Although a certain risk of failure will always remain the model predictions can be used to distinguish the existing cases of groundwater contamination between those which certainly have to be treated by active remediations measures and those cases where natural attenuation can be expected to reduce groundwater contamination to an acceptable level.

References

Acton, D.W. and Barker, J.F., 1992. In situ biodegradation potential of aromatic hydrocarbons in anaerobic groundwater. J. Contaminant Hydrol., 9(4): 325-353.

Barbaro, J.R., Barker, J.F., Lemon, L.A. and Mayfield, C.I., 1992. Biotransformation of BTEX under anaerobic, denitrifying conditions: Field and laboratory observations. J. Contaminant Hydrol., 11(3/4): 245-273.

Borden, R.C., Gomez, C.A. and Becker, M.T., 1995. Geochemical indicators of intrinsic bioremediation. Ground Water, 33(2): 180-189.

Cirpka, O.A., Frind, E.O. and Helmig, R., 1999. Numerical simulation of biodegradation controlled by transverse mixing. J. Contaminant Hydrol., 40(2): 159-182.

Cozzarelli, I.M., Herman, J.S. and Baedecker, M.J., 1995. Fate of microbial metabolites of hydrocarbons in a coastal plain aquifer: the role of electron acceptors. Environ. Sci. Technol., 29(2): 458-469.

Fried, J.J., Muntzer, P. and Zilliox, L., 1979. Ground water pollution by transfer of oil hydrocarbons. Ground Water, 17(6): 586-594.

Hadley, P.W. and Armstrong, R., 1991. "Where's the benzene?" - Examining California ground-water quality surveys. Ground Water, 29(1): 35-40.

Heron, G. and Christensen, T.H., 1995. Impact of Sediment-Bound Iron on Redox Buffering in a Landfill Leachate Polluted Aquifer (Vejen, Denmark). Environ. Sci. Technol., 29(1): 187-192.

Hindmarsh, A.C., 1974. GEAR : Ordinary differential equation solver. UCID-30001, Revision 3, Lawrence Livermore Laboratories, Livermore, Ca.

Holman, H.-Y.N. and Javandel, I., 1996. Evaluation of transient dissolution of slightly water-soluble compounds from a light nonaqueous phase liquid pool. Water Resour. Res., 32(4): 915-924.

HPC (Harress Pickel Consult GmbH), 1991. Veränderungen der hydrochemischen Milieubedingungen durch Zugabe einer KW-Quelle in einen Lockergesteinsaquifer, Gutachten im Auftrag der Deutsche BP AG, Abt. VS 4241, Hamburg, Kassel.

HPC (Harress Pickel Consult GmbH), 1992a. Bestimmung der Gesteinsdurchlässigkeiten und Ermittlung der Entnahmeraten für die Sanierungsbrunnen auf dem Aromatenfeld des

Terminal Ruhr der Deutsche BP AG in Hünxe, Gutachten im Auftrag der Deutsche BP AG, Abt. VS 4241, Hamburg, Kassel.

HPC (Harress Pickel Consult GmbH), 1992b. Verdichtende Untergrunderkundung und Sanierungsmaßnahmen im Bereich des ehemaligen Aromatenfeldes auf dem Gelände des Terminal Ruhr der Deutsche BP AG in Hünxe, Gutachten im Auftrag der Deutsche BP AG, Abt. VS 4241, Hamburg, Kassel.

Hunkeler, D., Höhener, P., Bernasconi, S. and Zeyer, J., 1999. Engineered in situ bioremediation of a petroleum hydrocarbon-contaminated aquifer: assessment of mineralization based on alkalinity, inorganic carbon and stable isotope balances. J. Contaminant Hydrol., 37(3-4): 201-223.

Imhoff, P.T., Jaffe, P.R. and Pinder, G.F., 1993. An experimental study of complete dissolution of a nonaqueous phase liquid in saturated porous media. Water Resour. Res., 30(2): 307-320.

Lovley, D.R., Woodward, J.C. and Chapelle, F.H., 1994. Stimulated anoxic biodegradation of aromatic hydrocarbons using Fe(III) ligands. Nature, 370: 128-131.

MacIntyre, W.G., Boggs, M., Antworth, C.P. and Stauffer, T.B., 1993. Degradation kinetics of aromatic organic solutes introduced into a heterogeneous aquifer. Water Resour. Res., 29(12): 4045-4052.

Montgomery, J.H. and Welkom, L.M., 1990. Groundwater chemicals desk reference. Lewis Publishers, Inc., Chelsea, MI, 640 pp.

Parkhurst, D.L., Thorstenson, D.C. and Plummer, L.N., 1980. PHREEQE - a computer program for geochemical calculations. U.S. Geological Survey.

Phillips, E.P., Lovley, D.R. and Roden, E.E., 1993. Composition of non-microbially reducible Fe(III) in aquatic sediments. Appl. Environ. Microbiol., 59(8): 2727-2729.

Powers, S.E., Abriola, L.M. and Jr., W.J.W., 1992. An experimental investigation of nonaqueous phase liquid dissolution in saturated subsurface systems: Steady state mass transfer rates. Water Resour. Res., 28(10): 2691-2707.

Powers, S.E., Abriola, L.M. and Weber Jr., W.J., 1994. An experimental investigation of nonaqueous phase liquid dissolution in saturated subsurface systems: Transient mass transfer rates. Water Resour. Res., 30(2): 321-332.

Schäfer, D., Schäfer, W. and Kinzelbach, W., 1998. Simulation of reactive processes related to biodegradation in aquifers 1. Structure of the three-dimensional reactive transport model. J. Contaminant Hydrol., 31(1-2): 167-186.

Schäfer, W. and Therrien, R., 1995. Simulating transport and removal of xylene during remediation of a sandy aquifer. J. Contaminant Hydrol., 19(3): 205-236.

Scheffer / Schachtschabel, 1998. Lehrbuch der Bodenkunde, Ferdinand Enke Verlag, Stuttgart

Therrien, R. and Sudicky, E.A., 1996. Three-dimensional analysis of variably-saturated flow and solute transport in discretely-fractured porous media. J. Contaminant Hydrol., 23(1-2): 1-45.

Thierrin, J., Davis, G.B. and Barber, C., 1995. A ground-water tracer test with deuterated compounds for monitoring in situ biodegradation and retardation of aromatic hydrocarbons. Ground Water, 33(3): 469-475.

Vroblesky, D.A. and Chapelle, F.H., 1994. Temporal and spatial changes of terminal electron-accepting processes in a petroleum hydrocarbon-contaminated aquifer and the significance for contaminant biodegradation. Water Resour. Res., 30(5): 1561-1570.

Zarda, B., Mattison, G., Hess, A., Hahn, D., Höhener, P. and Zeyer, J. , 1998. Analysis of bacterial and protozoan communities in an aquifer contaminated with monoaromatic hydrocarbons. FEMS Microbiology Ecology, 27(2): 141-152.

Parameter	Function	Value
k_{fx}, k_{fy}	horizontal hydraulic conductivity	173 m/d
k_{fz}	vertical hydraulic conductivity	69 m/d
I	local hydraulic gradient	0.07 %
Q (R41.2, R41.2, R41.4)	mean pumping rates of the 3 remediation wells	197 m^3/d, 184 m^3/d, 221 m^3/d
Q(R44.6, R44.8)	mean pumping rates of two adjacent wells	230 m^3/d, 285 m^3/d
Q_R	groundwater recharge rate	0.2 m/a
n_e	Effective porosity	25 %
α_L, α_{TH}, α_{TV}	longitudinal and transverse dispersivities	5 m, 0.1 m, 0.001 m
Γ	exchange coefficient between pore water and LNAPL	0.006 d^{-1} (slow exchange)
C_{sol}	Solubility of xylene	188 mg/l
R	retardation factor for xylene	2.9

Tab. 1: Flow and transport parameters used for the model calibration

Parameter	Function	Value	
		Aerobic bacteria	Denitrifying bacteria
v_{max}	maximum growth rate	0.1 d^{-1}	0.1 d^{-1}
v_{dec}	constant decay rate	0.01 d^{-1}	0.01 d^{-1}
MC_{xyl}	Monod-constant for xylene	2.2 mg/l	2.2 mg/l
$MC_{O, N}$	Monod-constant for oxygen and nitrate resp.	0.2 mg/l	0.5 mg/l
Y_{xyl}	Yield coefficient for xylene	0.1 g OC_{cell} / g OC_{xyl}	0.09 g OC_{cell} / g OC_{xyl}
ST_{xyl}	stoichiometric coefficient for xylene oxidation	3.2 g O_2 / g xylene	4.9 g NO_3 / g xylene
IC_O	Inhibition concentration for oxygen	-	0.05 mg

Tab. 2: Biochemical parameters for the aerobic and denitrifying bacteria

Parameter	Function	Value	
		sulfate reducers	iron reducers
v_{max}	growth rate	0.1 d^{-1}	0.1 d^{-1}
v_{dec}	constant decay rates	0.01 d^{-1}	0.01 d^{-1}
MC_{xyl}	Monod constant for xylene	22 mg/l	5.5 mg/l
$MC_{S, Fe}$	Monod constant for sulfate and iron resp.	70 mg/l	0.6 mg/l
Y_{xyl}	yield coefficient for xylene	0.02 g OC_{cell} / g OC_{xyl}	0.03 g OC_{cell} / g OC_{xyl}
ST_{xyl}	stoichiometric coefficient for xylene oxidation	4.8 g SO_4 / g xylene	22.1 g Fe / g xylene
IC_{Sauer}	inhibition concentration for oxygen	0.05 mg/l	0.05 mg/l

Tab. 3: Biochemical parameters for the sulfate and iron reducing bacteria

Figure Captions

Fig. 1: Location of the abandoned refinery together with a detailed view of the former xylene plant, the approximate extension of the spill (hatched zone), and the location of the sampling points. Groundwater discharges into the river Lippe, while the channel close to the refinery area is not hydraulically connected to the aquifer.

Fig. 2: Concentrations of the most important species recorded during groundwater and soil sampling in August 1990. The small dots in the figure for NAPL-xylene denote positions of sampling points used to delineate xylene distribution in the soil close to the water table. The larger dots in the other figures denote positions of the groundwater sampling points

Fig. 3: Model grid, extension of the LNAPL, and the locations of the three remediation wells. The central part of the model domain is fine-spaced with a distance of 10 m between the nodes and is surrounded by coarser cells in order to minimize boundary effects on simulation results. The largest spacing is 100 m.

Fig. 4: Measured and simulated xylene concentrations for the three remediation wells. The concentrations exhibit the typical trend for hydraulic remediation schemes with a pronounced decrease in concentrations during the first weeks of the well operations and only very gradually decreasing concentrations for later times.

Fig. 5: Simulated concentrations of sulfate and ferrous iron at the top of the aquifer for August 1990. For orientation the sampling points used for concentration interpolation of fig. 2 are also displayed.

Fig. 6: Location of the LNAPL-xylene in the regional model and positions of the six virtual observation points. The first observation point (P1) is located 100 m downstream the edge of the spill area, the second (P2) at 200 m distance and so on.

Fig. 7a: Concentration behaviour of xylene at the sampling points during the 24 years of simulation for non-reactive transport (scenario I). Xylene concentrations first rise to a maximum and then approach a plateau value. The concentrations slightly decrease in time

because the LNAPL is gradually removed when the spill area is flushed with groundwater from the uncontaminated upstream aquifer.

Fig. 7b: Temporal course of the xylene concentrations in the six sampling points for regional reactive transport conditions (scenario II). The concentration decrease along the flow path is much more pronounced than in scenario I (compare fig. 7a). Accordingly the concentration differences between the two scenarios are largest for the most downgradient observation point P6.

Fig. 8: Relative contribution of the different degradation pathways to total xylene degradation for the remediation period with wells in operation and for natural flow conditions

Fig. 9: Simulated xylene distribution for a vertical slice along the flow axis for both scenarios. While xylene has already migrated beyond the boundary of the model domain for the non-reactive case (top figure), it is permanently contained in a quasi-steady state plume for the reactive case (bottom figure).

Fig. 10: Simulated concentrations for selected reactive species of scenario II after 24 years of simulation for the same vertical slice as in fig. 9. At the top one can see the distribution of aerobic and denitrifying bacteria. The concentration distributions for dissolved oxygen, iron reducers and dissolved ferrous iron are shown beneath.

Fig.1

NAPL-xylene 100 m mg/kg

xylene mg/l

dissolved oxygen mg/l
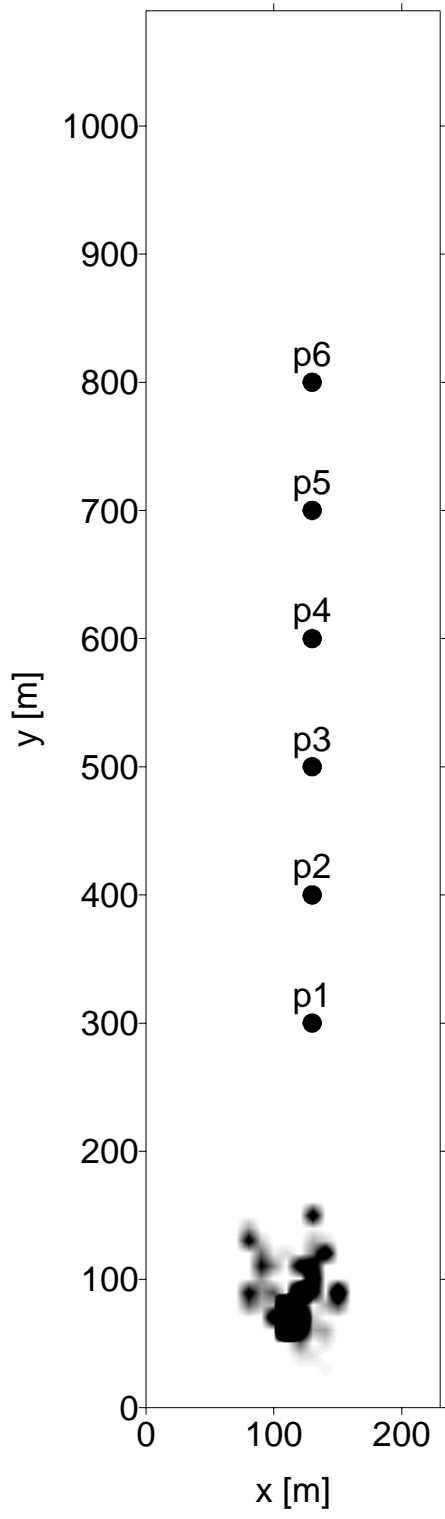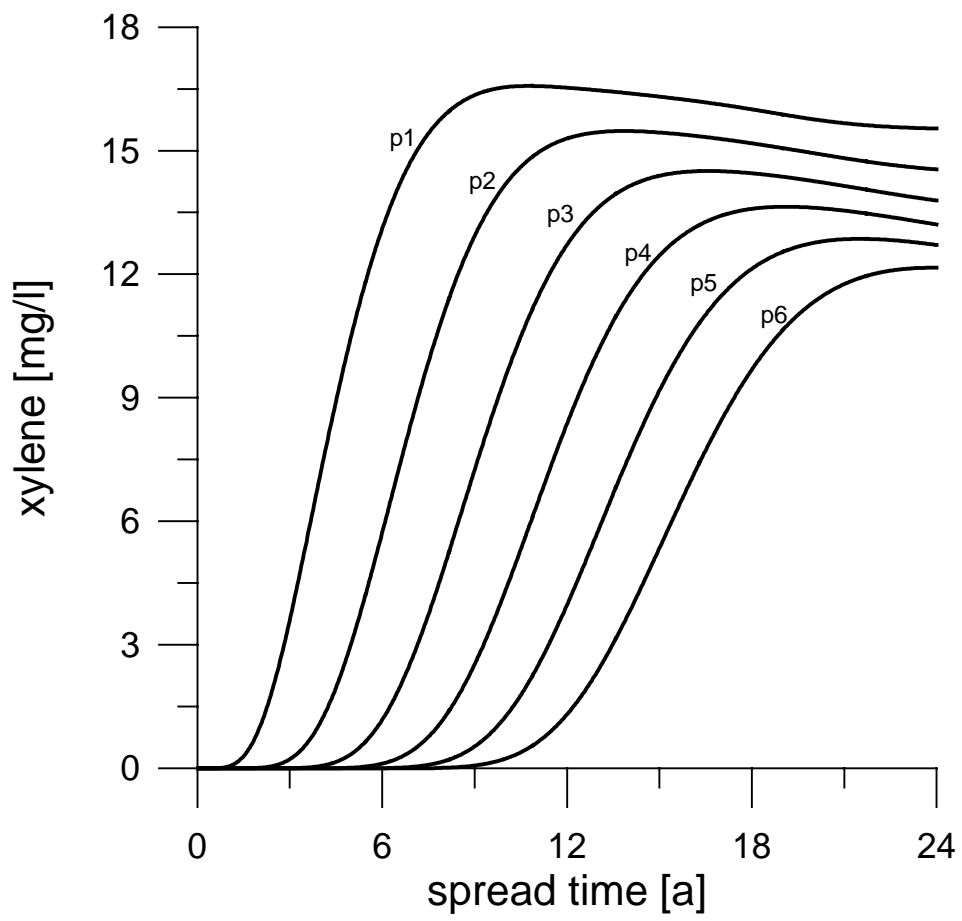
nitrate mg/l

sulfate mg/l

ferrous iron mg/l
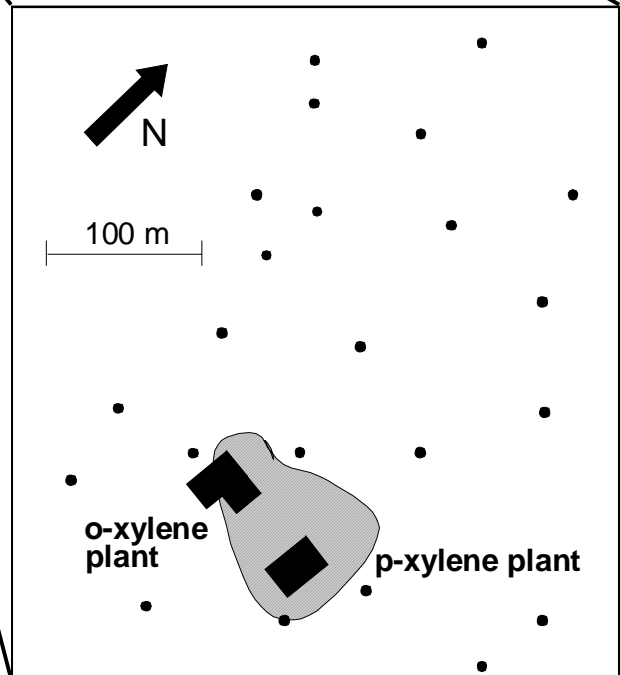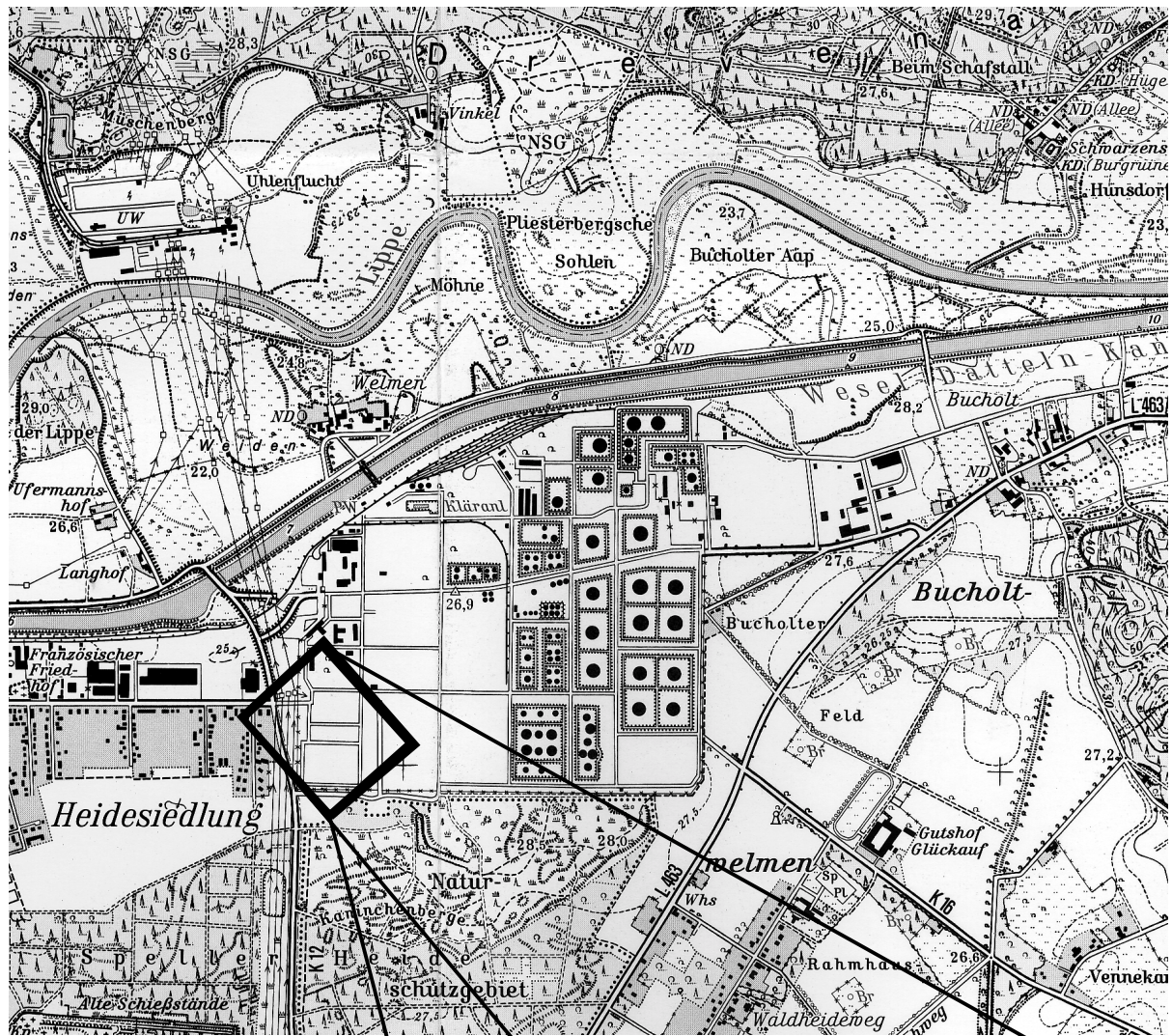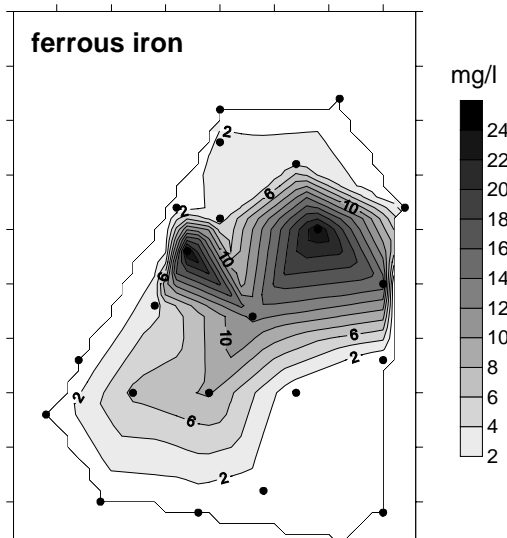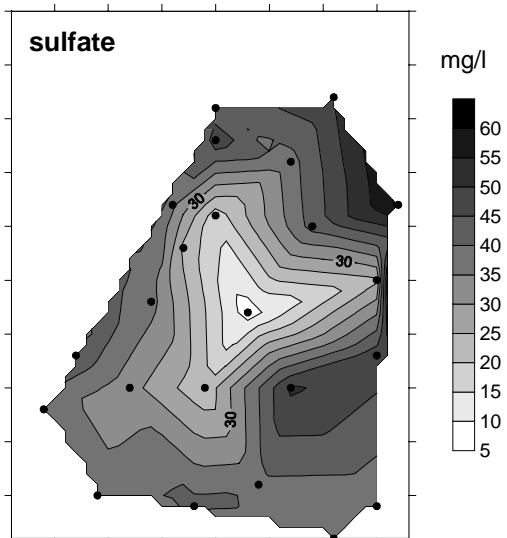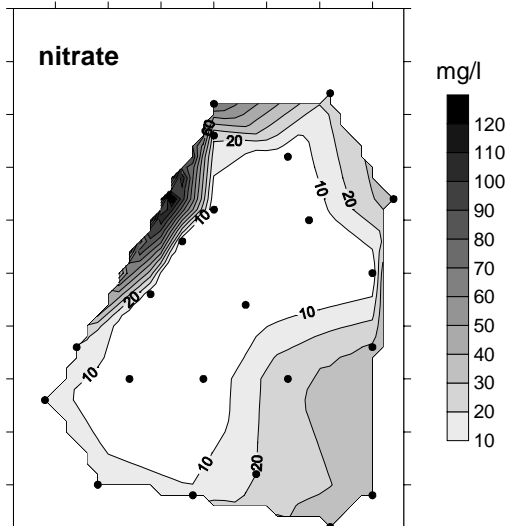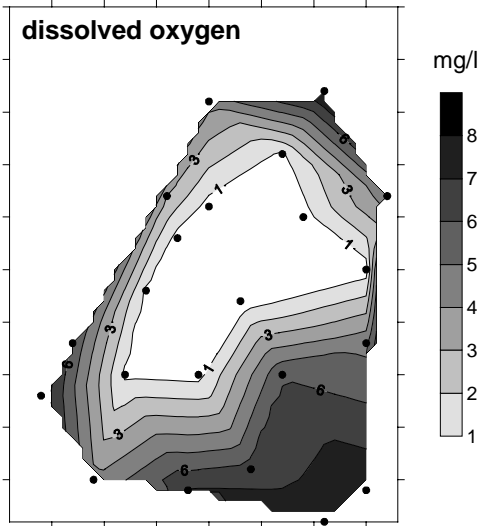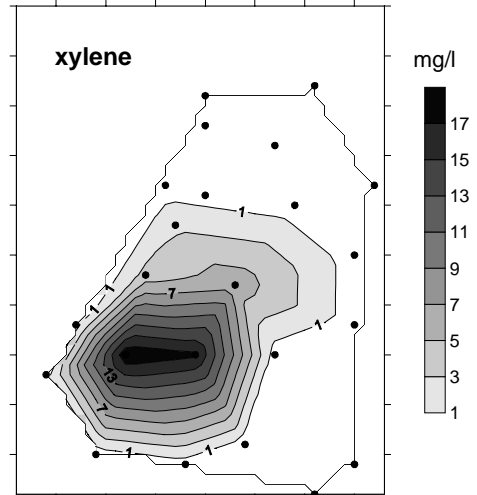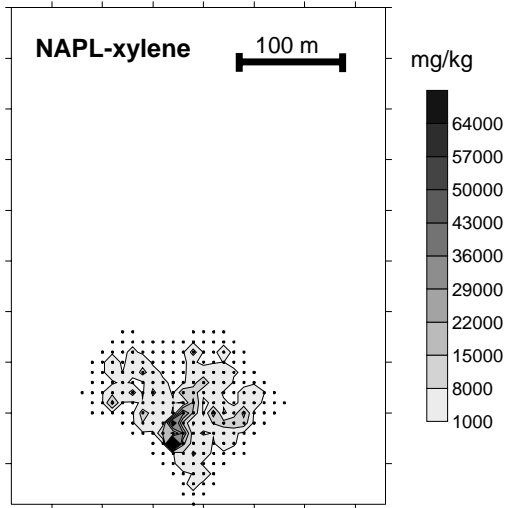
Fig.
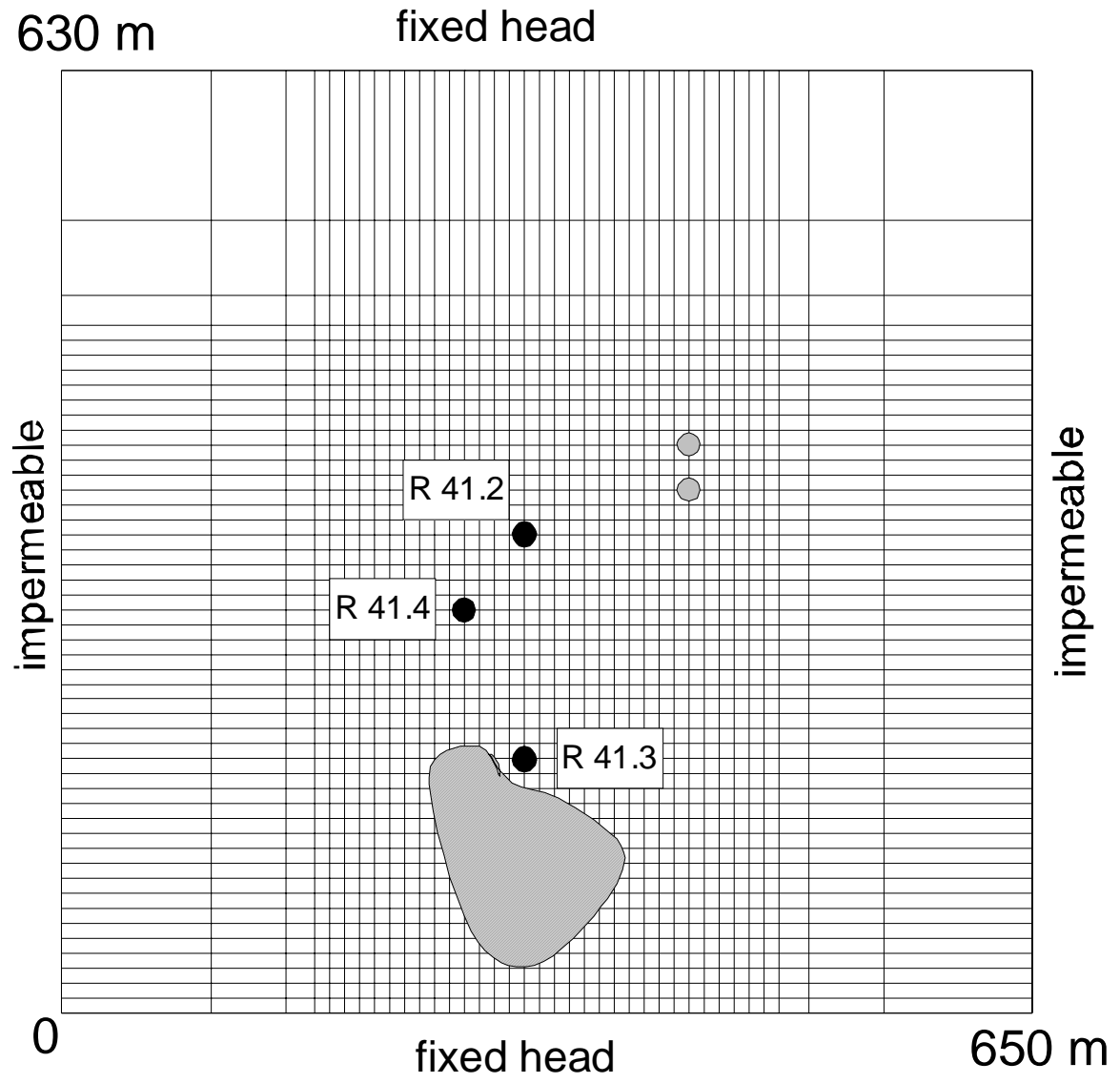
Fig. 3
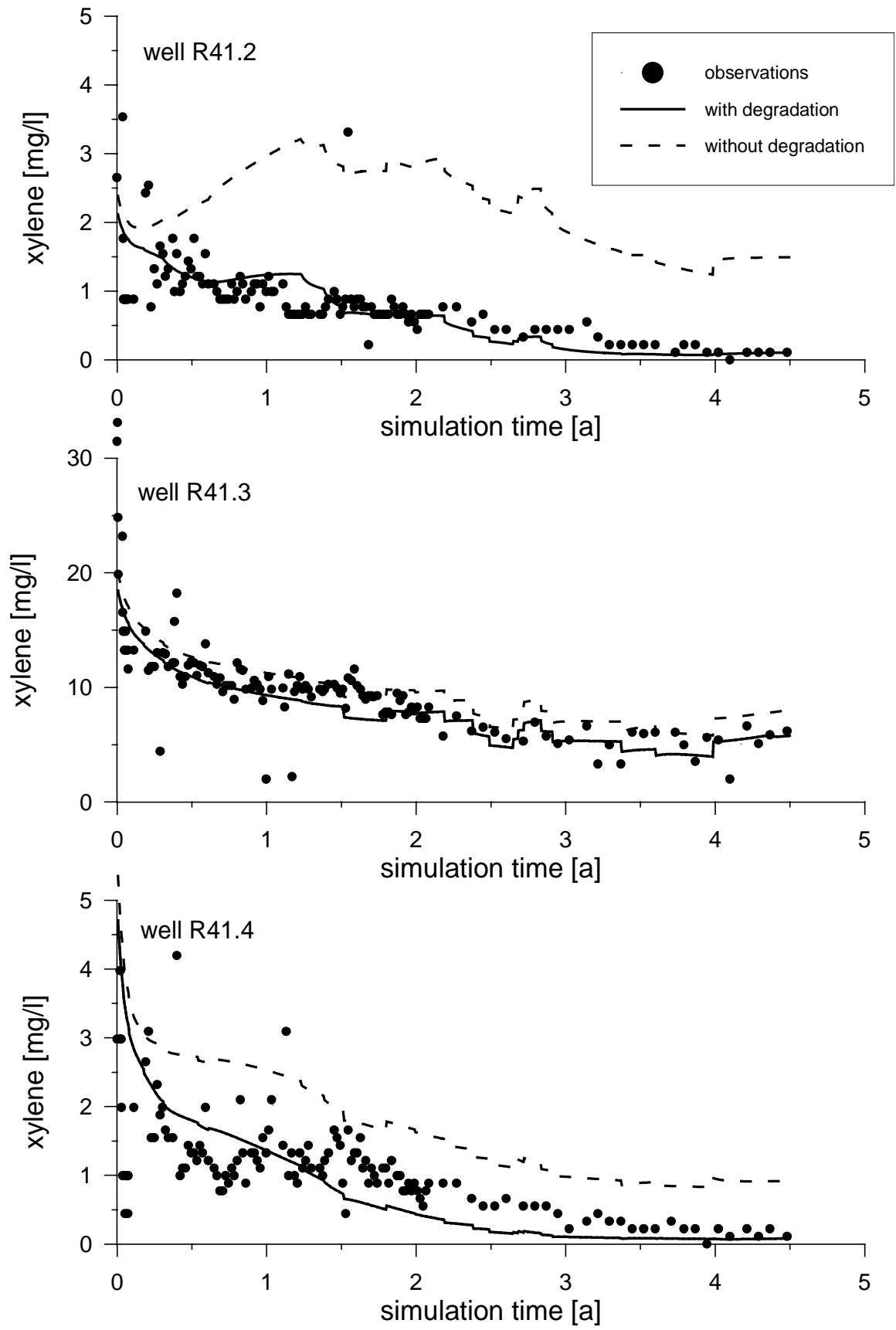
Fig. 4
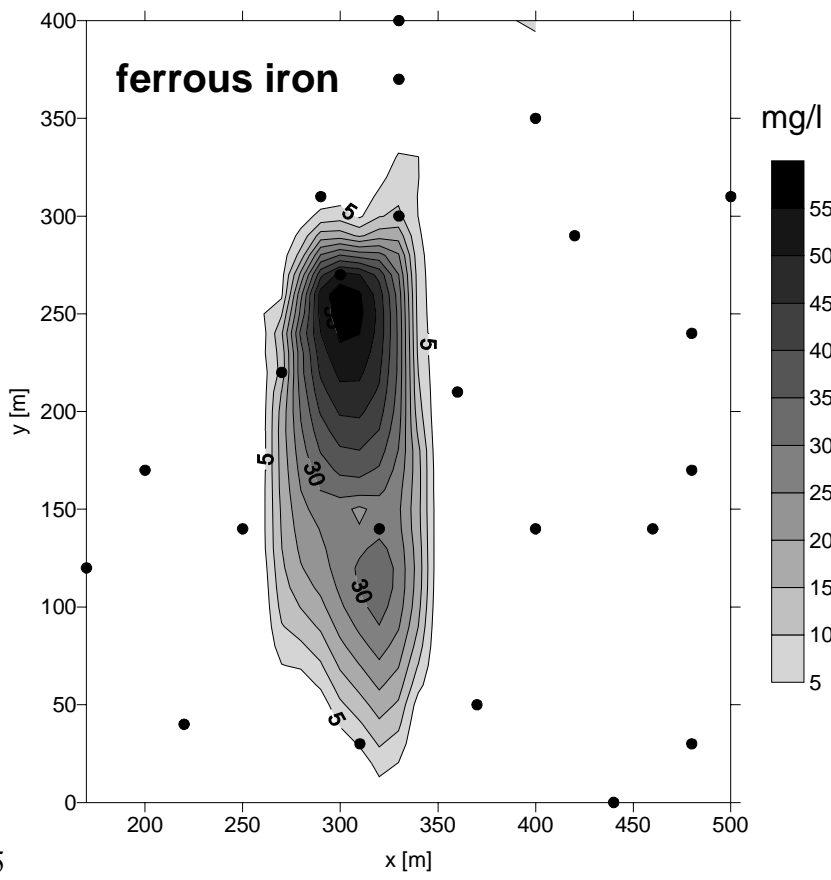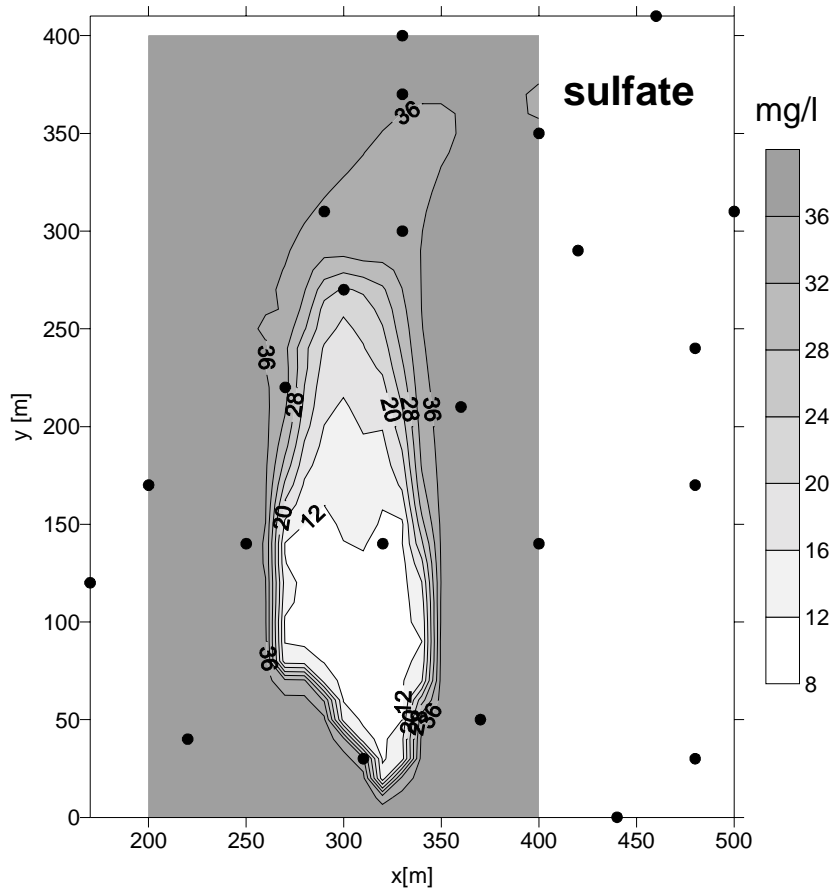
Fig. 5

Fig.6

Fig. 7a

Fig. 7b

Fig. 8

Fig. 9

aerobic and
denitrifying bacteria
[cells/g soil]

4.0E+004 1.2E+005 2.0E+005 2.8E+005 3.6E+005

dissolved oxygen
[mg/l]

0.5 1.0 1.5 2.0 2.5 3.0 3.5 4.0 4.5 5.0

iron reducers
[cells/g soil]

2.0E+003 6.0E+003 1.0E+004 1.4E+004

ferrous iron
[mg/l]

50 150 250 350 450

Fig. 10